Optical Detection of Tunneling Ionization

Aart J. Verhoef,[1] Alexander V. Mitrofanov,[1] Evgenii E. Serebryannikov,[2] Daniil V. Kartashov,[1] Aleksei M. Zheltikov,[2] and Andrius Baltuška[1]

[1]*Photonics Institute, Vienna University of Technology, Gusshausstrasse 27-29/387, A-1040, Vienna, Austria*

[2]*Physics Department, International Laser Center, M.V. Lomonosov Moscow State University, Vorobyevy gory, 119992 Moscow, Russia*

(Received 21 December 2009; published 23 April 2010)

We have experimentally detected optical harmonics that are generated due to a tunneling-ionization-induced modulation of the electron density. The optical signature of electron tunneling can be isolated from concomitant optical responses by using a noncollinear pump-probe setup. Whereas previously demonstrated tools for attosecond metrology of gases, plasmas, and surfaces rely on direct detection of charged particles, detection of the background-free time-resolved optical signal, which uniquely originates from electron tunneling, offers an interesting alternative that is especially suited for systems in which free electrons cannot be directly measured.

DOI: 10.1103/PhysRevLett.104.163904 PACS numbers: 42.65.Re, 32.80.Fb, 42.65.Ky

The interaction of an intense light field with matter results in a rich diversity of nonlinear-optical responses ranging from perturbative signals generated from a variety of nonlinear susceptibilities [1,2] to the higher-order harmonic generation (HHG) in the high-field regime [1,3]. The HHG phenomenon is one of the cornerstones of attosecond science and technology [4], enabling synthesis of attosecond soft x-ray pulses [5], probing of molecular orbitals [6], and control attosecond electron dynamics [7–9]. The physical mechanism behind the HHG, as insightfully explained by Corkum [10], involves the ionization of an electron by a strong laser field, acceleration of the free electron in the electric field of the laser pulse, and subsequent rescattering of this electron by a parent ion. The Corkum model excellently describes the experimentally measured plateau and cutoff higher-order harmonics and provides an important insight into the physics behind strong-field–matter interactions [3].

In the regime of tunneling ionization, an additional, physically different mechanism of optical harmonic generation is also possible. As shown by Brunel [11], with the ionization rate following the generic law of electron tunneling through a potential barrier in the dc limit, the plasma density displays extremely fast, nearly stepwise variations at every half-cycle of the laser field, causing the plasma current driven by an optical frequency of ω_0 to oscillate at the frequency $2\omega_0$. As a result, an optical field incident on this plasma will be dressed with frequency sidebands spaced at multiple $2\omega_0$ intervals, which we further refer to as tunnel-current harmonics. Detection of this type of nonlinear-optical response in the direction of the ionizing pulse is very challenging, because the tunneling current signal at harmonics order higher than ~9 is buried under the Corkum-type harmonics from the electrons rescattered off their parent ions, or under the harmonics originating from atomic and ionic susceptibilities at lower harmonic orders. To date, although some interesting and important experimental observations of the nonlinear wave mixing due to the Brunel-type modulation of the transverse plasma current have been reported [12,13], this regime of harmonic generation has never been experimentally disentangled from the other regimes of harmonic generation.

In this work, we employ a crossed-beam arrangement, depicted in Fig. 1, of a high-intensity linearly polarized few-cycle pump pulse and a weak cross-polarized probe pulse for a background-free detection of tunneling current optical harmonics. The approach demonstrated here recasts attosecond tunneling dynamics onto a slower, femtosecond

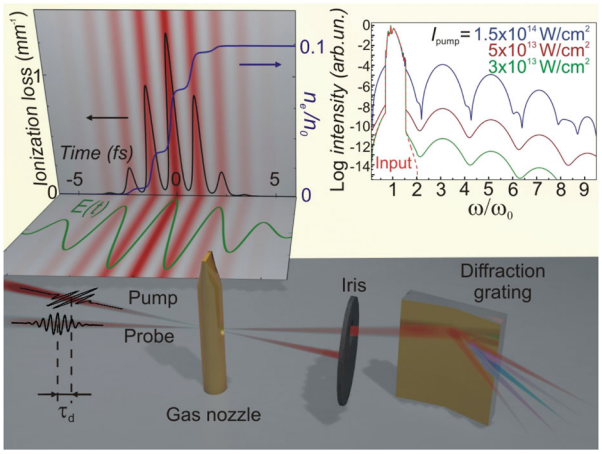

FIG. 1 (color). A high-intensity few-cycle pump pulse with a frequency ω_0 modulates the electron density through tunneling ionization. The pump field $E(t)$ (green line), its instantaneous intensity $[E(t)]^2$ (red stripes) and the calculated temporal profiles of the electron density (blue line) and ionization-induced loss (black line) are shown in the left panel. A weak noncollinear probe pulse applied with a variable time delay with respect to the pump reads out the pump-induced modulation of the plasma current, giving rise to odd-harmonic emission exactly along the probe-beam direction. The right panel displays the input laser field (dashed line) and the probe field with harmonics generated through plasma current modulation in the presence of a pump pulse with different intensities (encoded by different colors).

time scale of the interrogating optical probe pulse, paving the way toward an all-optical metrology of subcycle ionization dynamics. A significant advantage of using the Brunel emission mechanism is that, in contrast with the Corkum-type harmonic emission [10], it is free of the electron recombination step and, therefore, is not influenced by the final state of the electron. The quasiharmonic signals generated in this regime are controlled by attosecond ionization dynamics with their magnitude directly reflecting the rate of the electron release into the continuum.

The optical few-cycle pump pulse of a suitably high intensity suppresses the binding potential of an electron that can tunnel away from the ionic core through a field-modified, finite-width potential barrier within a time interval shorter than the field half-cycle. The rate of the electron ionization process, $w(t)$, is determined by the Keldysh parameter [14] $\gamma = \omega_0(2m_eI_p)^{1/2}(eE)^{-1}$, where ω_0 is the central frequency of the laser field, E is the field amplitude, I_p is the ionization potential, and e and m_e are the electron charge and mass, respectively. For large values of γ, multiphoton ionization dominates the ionization process, in which case $w(t)$ remains insensitive to the phase of the field. For low γ (typically $\gamma < 1$), ionization is dominated by electron tunneling. In this regime, the ionization rate $w(t)$ becomes highly sensitive to the phase of the field, peaking at the instants of time when the field intensity reaches its maximum. As a result, the electron density displays a steplike temporal profile, with each step corresponding to a respective field half-cycle (blue curve, Fig. 1, left). Such a behavior of the free electron plasma density $n_e(t)$ has been known from the earlier theoretical work (see Refs. [3,15] for an overview) and has been recently visualized experimentally in an elegant time-of-flight spectrometry measurement [8], where attosecond steps in the ion yield were detected using an isolated soft x-ray attosecond pump pulse and a few-cycle optical probe.

Exposed to a medium with a temporal modulation of the electron density, the optical probe (readout) field experiences time-domain phase modulation, $\Delta\Phi(t, z)$, and amplitude attenuation (plasma loss), $\alpha_p(t, z)$ (cf. Ref. [16] for full propagation model). Noteworthy is the fact that the interaction between the probe radiation and the plasma is a linear effect in terms of the probe field and is analogous to the interaction between the radio frequency carrier wave and the indirect frequency modulator employed in phase-modulation radio transmission.

The pump-induced plasma loss, proportional to $\alpha_p \propto I_p\partial n_e/\partial t$ [cf. the first term on the right-hand side of Eq. (S.1) in [16]], maps the temporal profile of $\partial n_e/\partial t$ onto the transmission of the probe field. In the regime of tunneling ionization, probe transmission becomes a pump-phase-sensitive pulsating function of time (black curve in Fig. 1, left), imposing an ultrafast, $\propto \partial n_e/\partial t$ amplitude modulation on the probe pulse (see Fig. S2.1 in Ref. [16]) and giving rise to odd-order harmonics of ω_0 in the spectrum of the probe field. The second frequency-transformation mechanism is related to the nonlinear phase shift $\Delta\Phi = \omega_0\delta n_p\Delta z/c$ of the probe field induced by an ultrafast modulation of the plasma current within a small propagation length Δz, with c being the speed of light in vacuum, $\delta n_p \approx -\omega_p^2/(2\omega_0^2)$, ω_p being the plasma frequency. Since $\omega_p^2 \propto n_e(t)$, this phase mask follows the temporal profile of $n_e(t)$ [cf. the last term on the right-hand side of Eq. (S.1) in [16]]. Because the stepwise changes in $n_e(t)$ are locked to half-cycles of the pump field, the phase-modulation mechanism also gives rise to quasiharmonic frequency peaks in the spectrum of the probe field (Fig. 1, right).

Therefore, the appearance of tunneling current emission in the probe spectrum is an unmistaken evidence of tunneling ionization which can be used to delineate the contributions of the tunneling and multiphoton ionization processes both leading to the $n_e(t)$ buildup. With an increase of the field intensity, the Keldysh parameter decreases, and electron tunneling becomes faster. This, in turn, increases the steepness of $n_e(t)$ steps, meaning that a faster electron tunneling results in a broader harmonic spectrum (Fig. 1, right). Following the logic of the Fourier series analysis, a set of measured multiple harmonic orders can be used to invert the frequency map of quasiperiodic tunneling into a time-domain evolution of plasma density n_e, provided the available number of Fourier components is suitably large. In view of the currently limited experimental precision, the task of full iterative inversion is beyond the scope of this paper.

The experimental approach adopted in this work is based on a noncollinear pump-probe arrangement sketched in Fig. 1. Linearly polarized pulses are split in two: one temporally compressed, 250 μJ, few-cycle ($\sim$5 fs) pump pulse and a weak slightly negatively chirped (duration $\sim$10 fs) probe pulse, with its polarization rotated by 90 degrees. Both pump and probe pulses are focused into a gas target with a length of 2.5 mm in the case of krypton and 1 mm in the case of argon. The gas pressure on target was set at 300 mbar in both cases. The pump and probe beam cross under an angle of about 1.5 degrees in the gas target (for more details, see [16]).

Several important comments are due on the measures to isolate the tunneling current emission spatially and temporally from contaminating signals. In the noncollinear pump-probe scheme used, the signal from the Corkum-type harmonics emitted in the pump beam direction is suppressed through the use of a different direction and polarization of the detection. By varying the pump-probe delay τ_d (Fig. 1) we are also able to discriminate between any possible background signal (at large positive or negative delay) due to atomic or ionic nonlinear susceptibilities, both instantaneous and delayed, and the signatures related

to tunneling ionization (around $\tau_d = 0$). Detection strictly in the probe direction, in addition, dismisses contamination from sum- and difference-frequency beams, because their phase-matched directions lie, correspondingly, inside and outside the pump-probe crossing angle. With this arrangement, we could reliably detect and perform reproducible frequency- and time-resolved measurements on the third, fifth, and seventh harmonics emitted from krypton and argon gas jets in the direction of the probe beam [Figs. 2(a)–2(c)]. These all-optical measurements represent the first background-free measurement of tunneling current emission and provide an addition to Ref. [8] experimental confirmation of the tunneling ionization occurring twice per optical cycle, as is manifested by $2\omega_0$ intervals [17] between the measured harmonic peaks.

As mentioned above, one of the properties of the observed optical signatures is the scaling law with the probe power, clearly distinguishing them from other nonlinear-optical responses. Figure 2(c) demonstrates that the frequency-integrated traces of the third, fifth, and seventh-order tunneling current harmonic maps follow, within the experimental precision, the convolution of the fundamental probe field with the amplitude mask given in Fig. 1, left (black curve), signifying that the temporal width

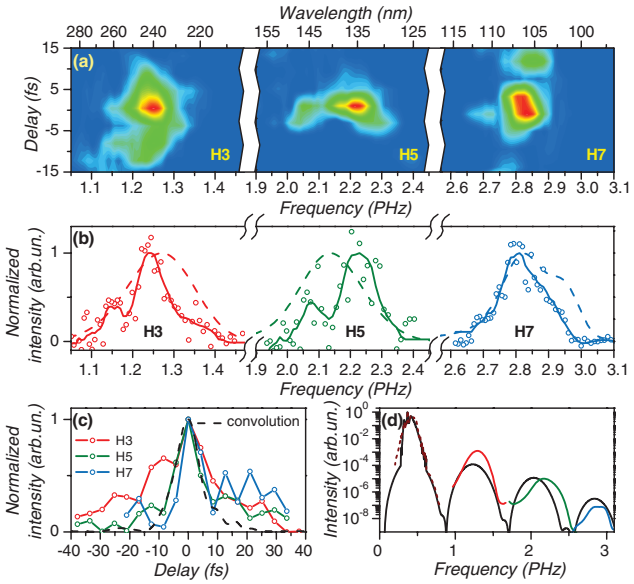

FIG. 2 (color). (a) Experimental maps of the third, fifth, and seventh harmonic of the probe beam detected as a function of delay between the pump and probe pulses from a 2.5 mm long krypton target. (b) Temporally integrated tunneling current harmonic signal spectra: measurement (solid lines) vs simulation (dashed lines). (c) The spectrally integrated harmonic signals as a function of pump-probe delay all show the same temporal structure, which agrees well to the calculated convolution of the amplitude mask with the probe pulse (dashed line). (d) Simulated tunneling harmonic spectra at zero pump-probe delay calculated without (black curve) and with the pulse propagation included (color coded curves).

does not scale with the harmonic order. A detailed study of probe power scaling in the case of the third harmonic in argon is summarized in Fig. 3. In the absence of the pump pulse, the probe pulse alone could also generate the third harmonic due to the atomic nonlinear susceptibility of the gas target in agreement with the $(W_{\mathrm{pr}})^3$ scaling with the energy W_{pr} of the probe field [Fig. 3(c), the $\times 10$ magnified red curve). With the pump field turned on, the third harmonic scaled linearly with the probe energy [black line in Fig. 3(c)], confirming our expectation following the analogy of frequency modulation on a radio frequency carrier.

The experimental time-frequency maps in Figs. 2(a) and 3(a) were analyzed using a full 3D few-cycle pulse propagation model in a rapidly ionizing gas. We use the pulse evolution equation written in the framework of the slowly evolving wave approximation [3,18] and adapted to include ionization effects [16,19,20]. Our model accounts for gas and plasma dispersion, diffraction, spatial self-action induced by the Kerr nonlinearity of the gas and plasma nonlinearity, spectral transformation phenomena, including self-phase modulation, wave mixing and harmonic generation, shock-wave effects, as well as ionization-induced loss and plasma-related nonlinear phenomena. The ionization rate $w(t)$ is calculated using the Yudin-Ivanov formula [21]. The predictive power of this model is illustrated by Figs. 2(b) and 3(a)–3(c) , which show that the results of simulations agree very well with the experimental data for the spectral and temporal properties of optical harmonics [Figs. 3(a) and 3(b)], as well as for the behavior of the third-harmonic signal as a function of the probe energy in the presence and in the absence of the pump field [Fig. 3(c)].

For the conditions of the experiments presented here, propagation effects in a tunneling-ionizing gas play a non-negligible role and influence both the pump and the probe pulses. An example of such distortion is presented

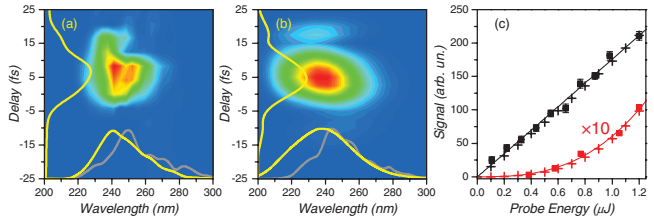

FIG. 3 (color). Experimentally measured (a) and simulated (b) spectrograms obtained from a 1 mm long argon target. The time integrated signal is collapsed on the spectral axis, and the spectrally integrated signal is collapsed on the delay axis (yellow lines). The experimentally measured signal below 220 nm is absorbed before the spectrometer. The grey lines show the normalized spectrum of the third harmonic in the absence of the strong pump pulse. Panel (c) shows the third-harmonic signal measured (■) and simulated (+) as a function of the probe energy in the presence of the strong pump pulse (black) and in the absence of the strong pump (red).

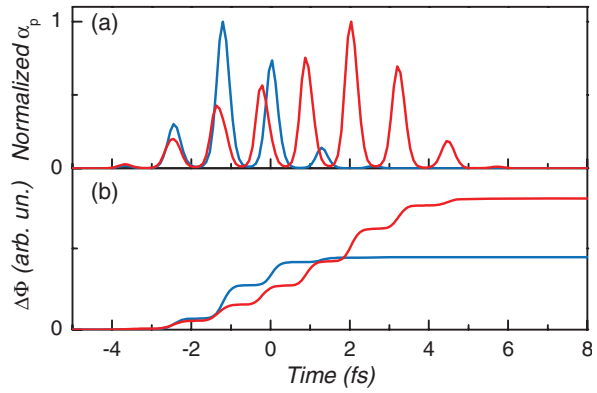

FIG. 4 (color). Amplitude (a) and phase (b) masks, correspondingly proportional to the time dependences of the ionization rate and the normalized electron density, in the tunneling current emission as a result of the interplay between the pump field and the pump-induced plasma, calculated on the beam axis at the input of the jet (blue curves) and at the position in the jet corresponding to the peak electron yield (red curves).

in Fig. 2(d), which shows numerically calculated tunneling current harmonic spectra at $\tau_d = 0$ for the pump field and the gas target used in our experiments in the case when the propagation effects in the plasma are disregarded (black curve) and when they are taken into account (color coded curves). The faster roll-off of the harmonic amplitudes and the shift of their center frequencies are attributed to the blurring of the amplitude and phase masks which is primarily caused by the evolution of the pump field traveling through the plasma target. Figure 4 shows the calculated amplitude and phase masks, corresponding to the initial propagation segment in the gas target and the masks at the propagation depth corresponding to the peak of electron yield. The reshaping of the tunneling current response as a function of propagation depth, gas pressure, and pump pulse intensity is examined in detail in Ref. [16]. The main conclusion of that analysis is that, despite an unavoidable distortion by the pump pulse evolution, the tunneling current emission mechanism is surprisingly robust. By increasing the pump pulse intensity or the gas target pressure, the ionization yield steeply increases, but the higher plasma density distorts the pump amplitude which in turn switches off the high tunnel ionization yield already a short distance into the target. As a result, the effective interaction length responsible for the tunneling current emission significantly shrinks while still yielding a spectral signature similar to the one seen at a lower target density or pump intensity.

In conclusion, we demonstrated an all-optical method enabling the detection of attosecond electron tunneling dynamics based on optical harmonic generation due to an ultrafast modulation of the plasma current in a fast-ionizing gas medium. This approach offers an all-optical alternative to the methods of attosecond metrology based on the detection of charged particles, allowing an extension of spectroscopic and imaging technologies capable of analyzing attosecond electron dynamics in large molecules and bulk solids. We have demonstrated that a noncollinear pump-probe experimental technique succeeds in separating the time-resolved maps of optical harmonics generated by tunneling electrons from optical signals originating from atomic and ionic nonlinear susceptibilities.

The authors thank M. Yu. Ivanov, O. Smirnova, and P. Corkum for fruitful discussions and R. Kienberger (Max-Planck-Institute of Quantum Optics, Garching, Germany) and A. Stepanov (Institute of Applied Physics, Russian Academy of Science, Nizhny Novgorod, Russia) for the kind loan of equipment. This research has been supported by the Austrian Science Fund (Grants No. U33-N16 and No. I185-N14), the Russian Federal Science and Technology Program (Contracts No. 1130 and No. 02.740.11.0223) and the Russian Foundation for Basic Research (Projects No. 09-02-91004, No. 09-02-12359, and No. 09-02-12373).

[1] A. L'Huillier *et al.*, *Nonlinear Optics, in Handbook of Lasers and Optics*, edited by F. Träger (Springer, New York, 2007), pp. 157–248.
[2] N. Bloembergen, *Nonlinear Optics* (Benjamin, New York, 1964).
[3] T. Brabec and F. Krausz, Rev. Mod. Phys. **72**, 545 (2000).
[4] P. B. Corkum and F. Krausz, Nature Phys. **3**, 381 (2007).
[5] E. Goulielmakis *et al.*, Science **320**, 1614 (2008).
[6] J. Itatani *et al.*, Nature (London) **432**, 867 (2004).
[7] A. Baltuska *et al.*, Nature (London) **421**, 611 (2003).
[8] M. Uiberacker *et al.*, Nature (London) **446**, 627 (2007).
[9] P. Eckle *et al.*, Science **322**, 1525 (2008).
[10] P. B. Corkum, Phys. Rev. Lett. **71**, 1994 (1993).
[11] F. Brunel, J. Opt. Soc. Am. B **7**, 521 (1990).
[12] N. Burnett, C. Kan, and P. B. Corkum, Phys. Rev. A **51**, R3418 (1995).
[13] C. W. Siders *et al.*, Phys. Rev. Lett. **87**, 263002 (2001).
[14] L. V. Keldysh, Zh. Eksp. Teor. Fiz. **47**, 1945 (1964) [Sov. Phys. JETP **20**, 1307 (1965)].
[15] W. M. Wood, C. W. Siders, and M. C. Downer, IEEE Trans. Plasma Sci. **21**, 20 (1993).
[16] See EPAPS supplementary material at http://link.aps.org/supplemental/10.1103/PhysRevLett.104.163904 for supplementary information.
[17] The appearance of odd harmonics in HHG spectra is determined by the twice-per-cycle periodicity of the recolliding trajectories of accelerated electrons rather than by the ionization mechanism alone.
[18] T. Brabec and F. Krausz, Phys. Rev. Lett. **78**, 3282 (1997).
[19] L. Bergé *et al.*, Rep. Prog. Phys. **70**, 1633 (2007).
[20] E. E. Serebryannikov, E. Goulielmakis, and A. M. Zheltikov, New J. Phys. **10**, 093001 (2008).
[21] G. L. Yudin and M. Yu. Ivanov, Phys. Rev. A **64**, 013409 (2001).